Integrated Micro-Computed Tomography and Computational Fluid Dynamics Analysis of Stepwise Enlargement in Mesial Root Canals of Mandibular Molars

Sofia Moura Furtado, DDS, MSc,[*] Jorge N. R. Martins, DDS, MSc, PhD,[†‡§]*
Emmanuel João Nogueira Leal Silva, DDS, MSc, PhD,[‖¶]
Mário Rito Pereira, DDS, MSc,[#]*
Marco Aurélio Versiani, DDS, MSc, PhD,[**] and
António Ginjeira, DMD, PhD[†]*

ABSTRACT

Introduction: To evaluate how stepwise enlargement in the mesial root canals of mandibular first molars affect shaping outcomes and irrigant dynamics. **Methods:** The shaping ability and irrigant flow patterns in mesial canals of mandibular first molars enlarged with ProTaper Next instruments (25/.06v, 30/.07v, 40/.06v) were evaluated using micro-computed tomography (micro-CT) and computational fluid dynamics (CFD). Instrument design and metallurgical properties were assessed by 3D scanning, scanning electron microscopy, energy-dispersive X-ray spectroscopy, and differential scanning calorimetry to ensure manufacturing consistency. An extracted mandibular molar with two curved mesial root canals was selected and scanned by micro-CT to generate 3D models for CFD simulation. Root canals were prepared stepwise with the ProTaper Next. Digital canal and needle geometries were reconstructed from micro-CT and scanning electron microscopy data. CFD simulations were conducted in ANSYS Fluent to calculate irrigant velocity, wall shear stress, and apical pressure. For shaping analysis, ten mesial canals from 5 mandibular molars were scanned before and after each preparation step. Canal volume, surface area, unprepared surfaces, and pericervical dentine thickness were quantified. Data were analyzed using repeated measures ANOVA with Bonferroni correction ($P < .05$). **Results:** Excluding for dimensions, all instruments shared similar metallurgical features and design characteristics, with minor surface imperfections. The open-ended needle consistently delivered irrigant to the working length, unlike the side-vented needle. Enlargement slightly increased apical velocity and irrigant density, particularly with the open-ended needle, which also generated higher wall shear stress and apical pressure. Canal volume and surface area increased significantly with larger files ($P < .05$), while unprepared areas decreased. Progressive canal enlargement significantly reduced minimal dentine thickness at the distal aspect of the mesial canals (most at 1–2 mm below the furcation), dropping from preoperative means of $\sim$1 mm to 0.60 mm after the 40/.06v instrument ($P < .05$), with the proportion of sections with dentine <0.5 mm increasing from 0% to 26%, while those >1 mm decreased markedly. **Conclusions:** Progressive apical enlargement improved shaping and irrigant dynamics, but additional increases offered limited benefits. Irrigant effectiveness was more influenced by needle design than by size alone, suggesting that optimizing delivery systems may enhance cleaning efficiency while minimizing unnecessary dentine removal. *(J Endod 2026;52:105–118.)*

KEY WORDS

Computational fluid dynamics; danger zone; dentine thickness; endodontics; irrigation flow; micro-computed tomography; shaping ability

SIGNIFICANCE

Progressive canal enlargement improved shaping and irrigation but caused significant dentine loss, especially in critical areas. Open-ended needles enhanced irrigant reach. Larger apical sizes boosted efficiency but increased weakening risk, highlighting the need for anatomy-tailored preparation.

From the *Faculdade de Medicina Dentária, Universidade de Lisboa, Lisboa, Portugal; †Grupo de Investigação em Bioquimica e Biologia Oral, Unidade de Investigação em Ciências Orais e Biomédicas (UICOB), Faculdade de Medicina Dentária, Universidade de Lisboa, Lisboa, Portugal; ‡Centro de Estudo de Medicina Dentária Baseada na Evidência (CEMDBE) - Cochrane Portugal, Faculdade de Medicina Dentária, Universidade de Lisboa, Lisboa, Portugal; §LIBPhys-FCT UID/FIS/04559/2013, Faculdade de Medicina Dentária, Universidade de Lisboa, Lisboa, Portugal; ‖School of Dentistry, Grande Rio University (UNIGRANRIO), Rio de Janeiro, Rio de Janeiro, Brazil; ¶Fluminense Federal University, Niteroi, Rio de Janeiro, Brazil; #Egas Moniz Center for Interdisciplinary Research (CiiEM), Egas Moniz School of Health & Science, Almada, Portugal; and **Dental Specialty

Root canal infection remains a leading cause of endodontic failure[1,2], highlighting the need for thorough cleaning and disinfection of the root canal system. This objective is often challenged by complex anatomical features, such as isthmuses, fins, and accessory canals, that are difficult to access with mechanical instruments and may harbor residual debris and microorganisms[3,4]. While mechanical preparation is essential for shaping the canal, effective irrigation is important for disinfecting areas that instruments cannot reach[5].

The primary function of irrigation is to remove debris, dissolve organic tissue, and eliminate microorganisms from the root canal space[6]. However, its effectiveness in reaching the apical third depends on several factors, including apical preparation size, irrigant flow rate, and needle design[7]. While larger apical diameters have been linked to improved irrigant penetration[8,9], enhanced debridement[10], and better clinical outcomes[11,12], excessive enlargement may compromise tooth structure and reduce its fracture resistance[13-15]. Excessive removal of dentine is especially critical in anatomically constrained areas such as the distal aspect of the mesial root of mandibular molars—the so-called danger zone—where the dentinal wall is thin and prone to perforation[16,17]. Pauletto et al.[14] demonstrated that increasing taper during canal preparation significantly compromises the biomechanical performance of mesial roots, while Smoljan et al.[15] showed that preserving pericervical dentine enhances the fracture resistance of mandibular molars. These findings highlight the importance of balancing the benefits of root canal enlargement with the preservation of dentinal structure, particularly in high-risk areas[18].

Advances in imaging technology, particularly micro-computed tomography (micro-CT), have significantly enhanced endodontic research by enabling high-resolution, nondestructive three-dimensional analysis of root canal morphology[19]. Micro-CT technology allows precise evaluation of the shaping ability of various nickel-titanium (NiTi) instruments by quantitatively assessing important morphometrical parameters such as dentine removal[17,20,21]. These detailed assessments provide critical insights for comparing instrumentation systems, refining preparation protocols, and optimizing treatment strategies to enhance clinical outcomes while preserving root structure integrity. Complementing micro-CT analysis, computational fluid dynamics (CFD) has become a key tool for investigating irrigant flow within the root canal system[7]. CFD simulations enable the assessment of clinically relevant variables, such as needle design, insertion depth, and apical preparation size, providing valuable insights into how these factors influence irrigant movement, penetration, and wall shear stress[22].

Although the morphology[23] and shaping[24] of mesial root canals in mandibular molars are well documented, integrating shaping analysis with CFD-based irrigation method would provide a more comprehensive view of how apical and canal enlargement affect both dentine preservation and irrigant effectiveness, advancing the development of more effective clinical protocols[20]. Therefore, this study evaluated how the stepwise enlargement of the mesial root canals of mandibular first molars affects shaping outcomes (canal volume, surface area, unprepared surfaces, and dentine thickness) and irrigant dynamics (velocity, wall shear stress, and apical pressure). The null hypothesis was that apical enlargement would not significantly influence these parameters.

MATERIAL AND METHODS

This manuscript protocol was approved by the local ethics committee (CE-FMDUL 202432).

Instrument Characterization

Before the experimental procedures, the design and metallurgical properties of the ProTaper Next instruments X2 (25/.06v), X3 (30/.07v), and X4 (40/.06v) (Dentsply Maillefer, Ballaigues, Switzerland) used in the stepwise preparation were analyzed to verify manufacturing consistency and exclude structural defects. This ensured that any differences observed after shaping could be attributed to instrument size rather than variability in production quality. The ProTaper Next X1 (17/.04v), used in the initial preparation phase according to the manufacturer's instructions, was not included in this analysis, since no shaping or irrigant-related parameters were assessed at this initial preparation size. Micro-CT measurements of the apical foramina from the selected mesial roots (DataViewer v.1.5.6.2; Bruker-microCT, Kontich, Belgium) revealed a mean diameter of 0.24 ± 0.11 mm. As the X1 tip size (0.17 mm) was smaller than the anatomical diameter of the canals, it's shaping ability and irrigant flow patterns were not evaluated.

One instrument of each type was scanned using a high-resolution optical 3D system (ATOS Q with 12 MP capsule MV40; GOM, Braunschweig, Germany). A 2 μm antireflective coating was applied under × 3.5 magnification using a precision airbrush to reduce reflections and scanning noise. Instruments were scanned at 12 MP from 24 angles over 360°, at a 290 mm working distance, covering a 40 × 40 × 40 mm volume. The point cloud was processed into triangulated STL meshes (GOM Inspect Suite 2020, GOM) to create 3D models. Cross-sections, instrument sizes, and blade volumes (tip to 18 mm) were analyzed using Geomagic Control X (3D Systems). Surface features and minor defects were also inspected by scanning electron microscopy (SEM) at 150 × (S-2400, Hitachi, Tokyo, Japan).

The metallurgical properties of each instrument type were analyzed using energy-dispersive X-ray spectroscopy (EDS) and differential scanning calorimetry (DSC). EDS was performed on three instruments of each type with a SEM (S-2400, Hitachi) and Inca X-act detector (Oxford Instruments, Abingdon, UK), operating at 20 kV and 3.1 A. Scans covered a 400 × 400 μm area for 60 s at a 25 mm working distance after a 10-min vacuum. Elemental ratios were calculated using ZAF correction and Microanalysis Suite v.4.14 (Oxford Instruments). DSC tests (DSC 204 F1 Phoenix; Netzsch, Selb, Germany) followed ASTM F2004-17 to[25] determine phase transformation temperatures. A 4–5 mm fragment (5–10 mg) was cut from each file, etched for 120 s in a solution of nitric acid (45%), hydrofluoric acid (25%), and distilled water (30%), then rinsed. Samples were placed in aluminum pans with an empty reference pan and run through a thermal cycle (−150°C to 150°C) at 10 °C/min under nitrogen for 1 h 40 min. Data were analyzed with Netzsch Proteus software.

Irrigation Analysis Using CFD

An extracted mandibular molar with two severely curved (37°) mesial root canals with a Vertucci Type II configuration was selected (Fig. 1*A*) from a pool of 327 permanent human mandibular molars that had been examined under a clinical microscope (M320 F12, Leica

Center, Brazilian Military Police, Belo Horizonte, Minas Gerais, Brazil

Address requests for reprints to Jorge N.R. Martins, Faculdade de Medicina Dentária da Universidade de Lisboa, Cidade Universitária, Lisboa 1649-003, Portugal.
E-mail address: jnr_martins@yahoo.com.br
0099-2399

https://doi.org/10.1016/j.joen.2025.09.001

Microsystems, Wetzlar, Germany) for root integrity. Roots with resorptive defects, cracks, open apices, or previous endodontically treated were excluded. Soft tissue remnants and calculus on the external root surface were removed by ultrasonic scaling (P5 Newtron XS; Satelec Acteon, Merignac, France). The distal root was excluded. The selected root was scanned using a micro-CT system (SkyScan 1275; Bruker-microCT) at 80 kV and 125 μA, with 19.61 μm resolution, 360° rotation, 0.5° steps, 58 ms exposure time, and frame averaging of 3, using a 1 mm aluminum filter. Images were reconstructed with NRecon v.1.7.3.1 (Bruker-microCT) and a STL model of the canals was created (CTAn v.1.20.8; Bruker-microCT) for numerical simulations.

After access opening, working length (WL) was set by inserting a size 10 K-file (Dentsply Maillefer) until visible at the apical foramen. The glide path was made manually with sizes 10, 15, and 20 K-files (Dentsply Maillefer), while root canal preparation was performed stepwise with ProTaper Next rotary instruments sizes X1 (17/.04v), X2 (25/.06v), X3 (30/.07v), and X4 (40/.06v) (Dentsply Maillefer). During preparation, canals were irrigated with 2 mL of 5.25% NaOCl. After enlargement to 25/.06v, a flat open-ended (NaviTip; Ultradent, South Jordan, UT, USA) and a side-vented (Max-i-Probe; Dentsply/Tulsa Dental, York, PA, USA) 30-G irrigation needles were tested to check if they could reach 3 mm and 1 mm short of WL without binding. Each tooth was scanned and reconstructed by micro-CT three times after enlargements to 25/.06v, 30/.07v, and 40/.06v using the same settings.

Three 3D root canal models, corresponding to preparation sizes 25/.06v, 30/.07v, and 40/.06v, were generated in STL format (CTAn v.1.20.8; Bruker-microCT) (Fig. 1*A*). Each model was standardized to 11 mm in length using SolidWorks 2017 (Dassault Systèmes, Paris, France). Digital models of flat open-ended and side-vented irrigation needles were created based on SEM images (Vega3-LMU, TESCAN, Kohoutovice, Czech Republic) of a 30G NaviTip (Ultradent) and a 30G Max-i-Probe (Dentsply/Tulsa Dental), with outer and inner diameters of 320 μm and 170 μm, respectively. Needles were 25 mm long, with tips placed 3 mm (flat) and 1 mm (side-vented) short of the WL. All models were imported into ANSYS 2019 R2 (ANSYS, Canonsburg, PA, USA), and six flow domains were built to reflect the combinations of preparation size, needle type, and depth. Tetrahedral meshes with prism layers and near-wall refinement were generated using the ANSYS meshing module. Final meshes, verified for independence, contained 6.2–7.6 million elements.

Flow simulations were run in ANSYS Fluent using a 3D, incompressible, pressure-based transient solver. Laminar flow was assumed, based on a validated model[26]. Continuity and momentum equations were solved using the SIMPLE algorithm. A velocity of 0.1 mL/s was applied at the needle inlet. The irrigant (2.5% NaOCl) was treated as an incompressible Newtonian fluid ($\rho = 1060$ kg/m^3, $\mu = 1.073 \times 10^{-3}$ Pa s)[27]. Atmospheric pressure was set at the canal outlets, and canal walls were rigid, impermeable, and followed a no-slip condition. A second-order upwind scheme was used for momentum convection, with second-order discretization for velocity terms. Time was integrated using a second-order implicit scheme with a 10 μs step over 1 s. Initial conditions assumed zero velocity ($u = 0$) and uniform pressure ($P = 0$). Simulations converged when residuals dropped below 0.001. At the end of the simulations, CFD-Post was used to analyze flow patterns, irrigant velocity, wall shear stress, and apical pressure for each flow domain. Simulations were run on a workstation with a 24-core Intel Xeon 2.4 GHz processor and 128 GB of RAM.

Shaping Ability - Unprepared Canal Walls

Sample size calculation was based on the percentage of static voxels (unchanged areas after canal enlargement), using data from the two mesial root canals previously analyzed in the CFD simulations. These canals had a Vertucci Type II configuration and were prepared using the same stepwise protocol and micro-CT scanning settings adopted for the current assessment. With $\alpha = 0.05$, power = 80%, effect size = 11.15, and SD = 6.58, the estimated sample size was seven canals per group. To ensure statistical reliability and account for potential variability, a total of ten mesial canals were included. Two mesial canals previously used in the CFD analysis were included, and eight additional canals from four mandibular molars with similar anatomy were prepared under identical conditions, using the same instrumentation sequence and imaging protocol.

Prepreparation and postpreparation scans were coregistered using 3D Slicer 4.3.1 (http://www.slicer.org) to generate 3D models for quantitative analysis (CTAn v.1.20.8; Bruker-microCT). Intracanal volume (mm^3) and surface area (mm^2) were measured separately for each mesiobuccal (MB) and mesiolingual (ML) canal. The percentage of unprepared canal walls was calculated for the entire mesial root canal system as the percentage of static surface voxels using the formula: (SVn × 100)/SVt, where SVn represents the number of unchanged surface voxels and SVt the total surface voxel count[28].

Shaping Ability - Dentin Thickness

CTAn v.1.20.8 (Bruker-microCT) was also used to create 3D dentine thickness maps, while CTVox v.3.3.1 (Bruker-microCT) supported qualitative assessment before and after each preparation step. Color-coded cross-sections were used to measure (in mm) the minimum dentine thickness on the distal aspect (danger zone) of the MB and ML canals at the furcation level and up to 4 mm towards the apical direction (pericervical region). Three measurements were taken at each level and averaged. Then, dentine thickness values were categorized as <0.5, 0.5– 1.0, and > 1.0 mm, and their percentage frequencies calculated. All analyses were performed by a micro-CT expert blinded to the preparation protocols.

Statistical Analysis

Normality of the data for intracanal volume, surface area, dentine thickness, and unprepared canal areas was confirmed using the Shapiro-Wilk test ($P > .05$), and these variables were reported as means and standard deviations. Group comparisons, including preoperative values and those following sequential preparations with 25/.06v, 30/.07v, and 40/.06v instruments, were performed using repeated measures ANOVA with Bonferroni *post hoc* correction. Statistical significance was set at $P < .05$ (SPSS v.22 for Windows; IBM SPSS Statistics, Chicago, IL, USA).

RESULTS

Instrument Characterization

The 3D surface scanning showed that all instruments shared the same off-center rectangular cross-section. Their only difference was size, confirmed by qualitative evaluation and quantitative analysis of volume (25/.06v: 5.69 mm^3; 30/.07v: 6.82 mm^3; 40/.06v: 7.77 mm^3). SEM images revealed similar surface finishes with parallel machining marks and minor irregularities, including slight rollovers on all instruments. EDS confirmed a near-equiatomic NiTi alloy (25/.06v: 1.026; 30/.07v: 1.018; 40/.06v: 1.021) with no other metals detected. DSC analysis showed consistent phase transformation temperatures across instruments (R-phase start: 45 °C; R-phase finish: 15 °C; austenite start: −5 °C; austenite finish: 50 °C) (Fig. 2).

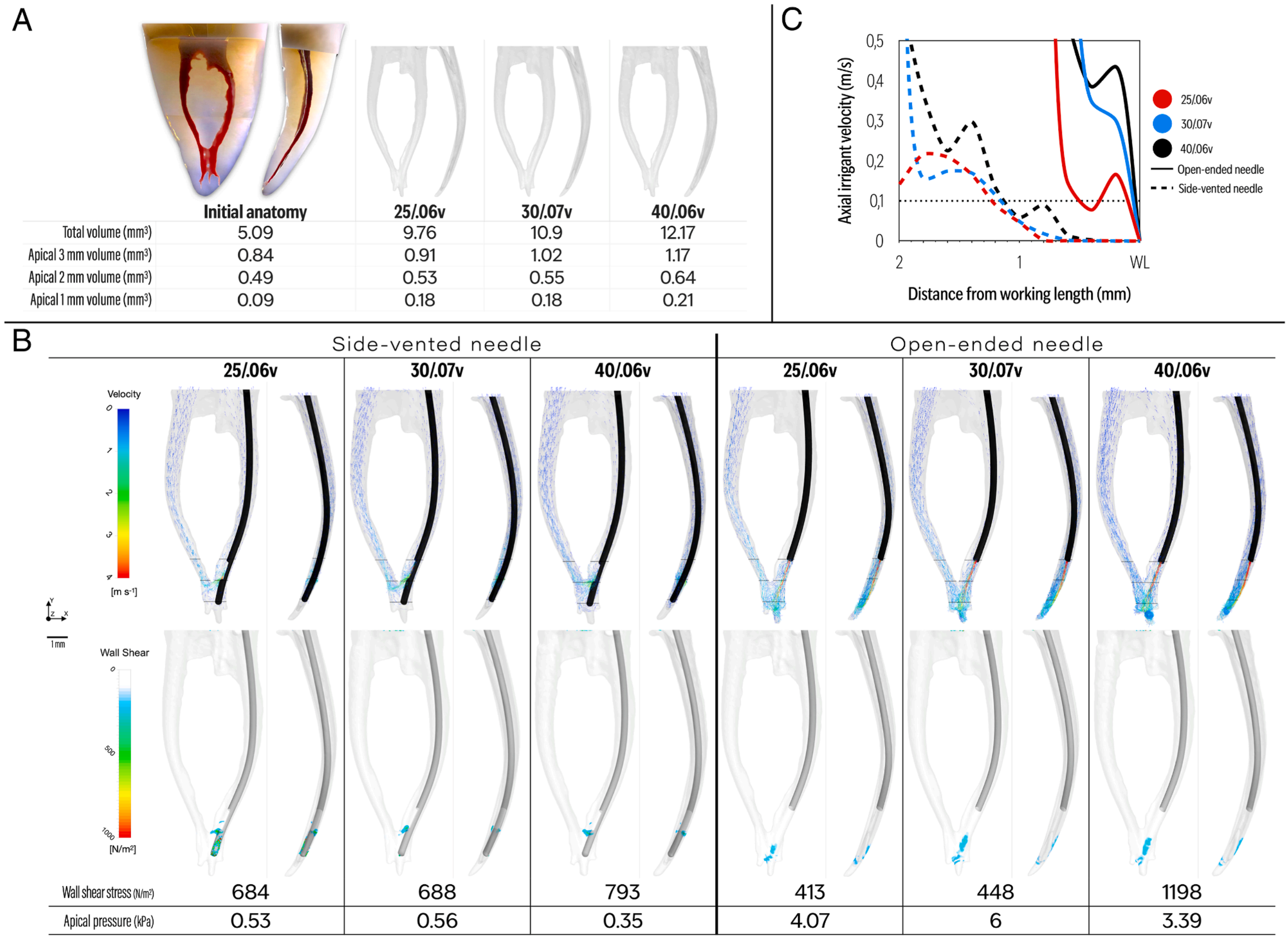

FIGURE 1 – Computational fluid dynamics (CFD) assessment. (*A*) Proximal and clinical views of the 3D reconstruction of the mesial root showing the initial canal anatomy and the geometry after mechanical preparation with instruments 25/.06v, 30/.07v, and 40/.06v. Total and apical volumes (1 mm, 2 mm, and 3 mm segments) are shown in mm^3. (*B*) Proximal and clinical views of velocity vectors along streamlines illustrating the direction and magnitude of irrigant flow (at t = 1 s, top row), time-averaged wall shear stress contours (second row), maximum wall shear stress (N/m^2), and mean apical pressure (kPa) for both side-vented and open-ended needles placed 1 mm and 3 mm short of the working length, respectively, across all preparation sizes. (*C*) Maximum time-averaged axial irrigant velocity within the apical 2 mm of the canal as a function of distance from the working length for each needle and preparation size. The vertical axis is scaled 0–0.5 m/s to emphasize differences in the region apical to the needle tip. Colored dots on the horizontal axis indicate the needle tip position. Velocities exceeding 0.1 m/s (dotted line) were considered to reflect clinically relevant penetration.

Irrigation Analysis Using CFD

CFD simulation results are shown in Fig. 1*B* and *C*. Once each needle's characteristic jet was established, flow diverted toward the canal orifices, mainly through the confluent canal opposite the needle. Apical irrigant delivery varied by needle type: the open-ended needle consistently reached the WL in all scenarios, while the side-vented needle did not. Increasing the preparation size had minimal effect on flow patterns or apical penetration but slightly increased apical irrigant density. With the open-ended needle, irrigant reached the apex even in the 25/.06v preparation, and apical velocity increased after enlargement to 30/.07v. Both needles maintained similar wall shear stress patterns, but the open-ended design produced higher stress along the outer curvature. Shear stress magnitude increased slightly with larger preparations. Apical pressure was consistently lower with the side-vented needle, and although no clear trend emerged with increasing enlargement size, the 40/.06v preparation yielded the lowest pressure for both needle types.

Shaping Ability - Unprepared Canal Walls

Results of intracanal volume, surface area, and unprepared canal surface are summarized in Table 1. Intracanal volume and surface area increased significantly with each instrument size, from the lowest values with 25/.06v to the highest with 40/.06v ($P < .05$). The percentage increase of volume was smaller between the 30/.07v and 40/.06v than in earlier steps. The mean percentage of unprepared canal walls significantly decreased from 18.07% with the 25/.06v instrument to 8.72% with the 30/.07v and 7.15% with the 40/.06v ($P < .05$). However, none of the instruments achieved complete preparation of all canal walls (Fig. 3).

Shaping Ability - Dentin Thickness

Color-coded 3D models revealed progressive dentine thinning, mainly along the distal aspect of the mesial root (danger zone) (Fig. 3). At 1 mm below the furcation, the mean minimal dentine thickness of the MB canal significantly decreased from 0.99 mm (preoperative) to 0.76 mm after preparation with the 25/.06v, 0.66 mm with the 30/.07v, and 0.60 mm with the 40/.06v instrument ($P < .05$). A similar trend was observed in the ML canal, where mean dentine thickness

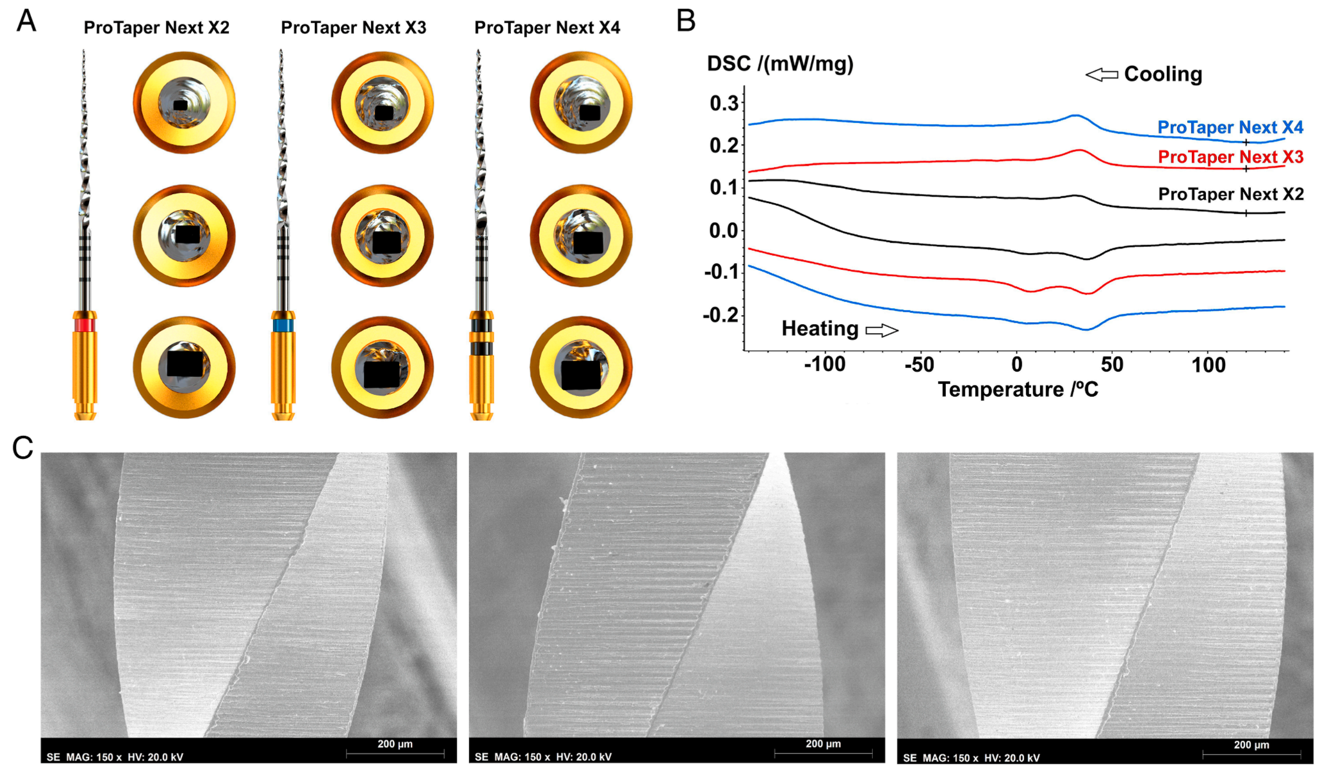

FIGURE 2 – Instrument characteristics. (*A*) 3D surface scans showed similar designs across instruments, with identical and consistent cross-sectional geometry along the active blade length; only the cross-sectional dimensions differed. (*B*) Differential scanning calorimetry charts indicated comparable phase transformation temperatures for all instruments. (*C*) Scanning electron microscopy revealed similar surface finishes, with parallel machining marks and few surface irregularities.

reduced from 1.01 mm to 0.74 mm (25/.06v), 0.65 mm (30/.07v), and 0.60 mm (40/.06v) ($P < .05$). This progressive thinning at the distal root aspect was noticed also at the furcation level and continued at the 2 mm, 3 mm, and 4 mm levels in both canals, though the reduction was most pronounced at the 1 mm and 2 mm level (Table 2). Before preparation, most cross-sections in the MB (56%) and ML (48%) canals had dentine thicker than 1 mm. After the 25/.06v instrument, these values dropped to 34% and 28%, and further decreased to 12% and 8% after preparation with the 40/.06v instrument. In contrast, sections with dentine between 0.5–1.0 mm increased after the sequential steps, reaching more than 60% for both canals. No sections had dentine thinner than 0.5 mm before preparation, but this number increased with each step, reaching 26% in both canals after the final enlargement (Table 3; Fig. 4).

DISCUSSION

Effective infection control in endodontic therapy relies on thorough root canal cleaning and disinfection, which are intrinsically linked to the quality of canal shaping[29] and the dynamics of irrigant delivery[30], particularly in anatomically complex regions such as the mesial roots of mandibular molars. This study evaluated the impact of stepwise apical enlargement using 25/.06v, 30/.07v, and 40/.06v ProTaper Next instruments on both shaping outcomes and irrigant flow behavior, by integrating micro-CT and CFD. To the best of the authors' knowledge, this is the first investigation to combine these methodologies to explore how preparation size and taper influence irrigation efficacy and dentine preservation in mesial root canals. The results demonstrated that progressive enlargement improved canal shaping and wall shear stress but also caused a significant reduction in dentine thickness in the pericervical region. A key aspect is not only identifying the direction of these effects but also quantifying their magnitude, as this determines whether the observed differences meaningfully influence the clinical decision when balanced against dentine preservation and irrigation performance. These findings underscore the need to balance effective disinfection protocols with the preservation of structural integrity. Accordingly, the null hypothesis was rejected, as root canal enlargement significantly influenced both shaping characteristics and irrigant performance. In agreement with ElAyouti et al.[31], the apical foramen was adopted as the most consistent apical reference for determining WL, as it represents the external anatomical landmark and may coincide with the pulp–periodontal junction. Therefore, in this *ex vivo* design, establishing WL by visualizing the file tip at the major foramen ensured a standardized and reproducible reference across all specimens.

Although numerous studies have investigated root canal shaping[24], there remains no consensus regarding the optimal apical size or taper for canal preparation[11]. Nonetheless, emerging evidence indicates that both parameters are critical for enhancing the efficacy of chemo-mechanical debridement. Specifically, an apical preparation size of ≥30 has been recommended to improve microbial reduction and facilitate deeper penetration of irrigants into the complex anatomy of the root canal system[12]. Adequate tapering also plays a key role by promoting effective irrigant exchange and distribution along the entire WL, thereby improving disinfection outcomes[30]. However, this must be balanced against the risk of excessive dentine removal, which can weaken root structure and increase susceptibility to procedural complications such as strip perforation or vertical root fracture[32,33]. Therefore, the choice of instrument size and

TABLE 1 - Mean and Standard Deviation [Minimum and Maximum] of Intracanal Volume, Surface Area, and Unprepared Canal Areas (% of StaticVoxels) Before and After Sequential Root Canal Enlargement

Parameter	Preoperative	25/.06v	30/.07v	40/.06v
Mesiobuccal canal				
Volume (mm^3)	1.75[a] ± 0.69 [0.71-2.66]	3.24[b] ± 0.71 [2.07-4.25]	3.78[c] ± 0.65 [2.98-5.17]	4.12[d] ± 0.66 [3.06-5.40]
Volume increase (%)	—	103.53 ± 60.32 [27.71-201.41]	18.68 ± 15.55 [0.57-46.38]	9.36 ± 6.21 [0.99-18.46]
Surface area (mm^2)	21.38[a] ± 5.20 [13.46-28.11]	26.33[b] ± 3.98 [20.71-31.78]	28.36[c] ± 3.48 [23.28-34.67]	29.42[d] ± 3.25 [25.06-35.38]
Area increase (%)	—	26.49 ± 18.35 [8.38-66.05]	8.43 ± 8.72 [0.68-29.70]	3.93 ± 3.06 [0.19-8.10]
Mesiolingual canal				
Volume (mm^3)	1.76[a] ± 0.66 [0.53-2.67]	3.32[b] ± 0.56 [2.29-3.97]	3.84[c] ± 0.52 [3.01-4.68]	4.22[d] ± 0.65 [3.03-4.86]
Volume increase (%)	—	120.72 ± 118.07 [33.33-435.85]	16.97 ± 11.27 [0.55-31.44]	9.66 ± 6.04 [0.66-18.92]
Surface area (mm^2)	21.71[a] ± 3.97 [15.74-27.71]	25.93[b] ± 3.40 [20.55-30.41]	27.66[c] ± 3.33 [23.06-33.89]	28.86[d] ± 3.28 [24.73-34.41]
Area increase (%)	—	21.13 ± 15.09 [5.90-49.68]	6.98 ± 5.88 [0.23- 20.00]	4.45 ± 3.61 [0.28-10.97]
Mesial root canal system				
Unprepared canal walls (%)	—	18.07[a] ± 8.47 [6.69-32.16]	8.72[b] ± 4.85 [2.89-18.24]	7.15[c] ± 4.70 [2.11-16.04]

Different superscript letters in each line represent statistically significant differences between instruments ($P < .05$).

taper should be informed by a comprehensive understanding of root canal anatomy, supported by clinical judgement and current evidence. In this context, the present study demonstrated that varying apical enlargement sizes significantly influenced parameters related to shaping performance and dentine preservation, reinforcing the importance of selecting a preparation protocol that balances cleaning efficacy with structural integrity.

The present study confirmed that all tested ProTaper Next instruments had identical design characteristics and metallurgical properties, differing only in their tip size and taper. Each instrument featured the same off-centered parallelogram cross-section and exhibited a uniform surface finish with minimal machining irregularities (Fig. 2*B*). No structural defects or design inconsistencies were identified. EDS analysis demonstrated a nearly equiatomic NiTi composition, with no detectable traces of additional metallic elements. Furthermore, DSC test (Fig. 2*C*) revealed highly comparable phase transformation temperatures among the instruments, indicating similar thermomechanical behavior. Collectively, these findings support the conclusion that the observed differences in shaping outcomes across instruments are applicable exclusively to variations in size and taper, rather than differences in material composition or manufacturing quality.

The shaping ability of NiTi instruments is critical in endodontics, as it directly affects canal cleaning efficacy, anatomical preservation, structural integrity, and obturation quality, while also enhancing irrigant penetration, debris removal, and minimizing procedural errors, all of which contribute to long-term treatment success[34]. Currently, there is growing emphasis on minimally invasive techniques in endodontics, with particular attention to preserving pericervical dentine, the critical 4 mm of dentine located both coronally and apically to the crestal bone level[35]. This region has been associated with the structural integrity of endodontically treated teeth, and although its precise role remains debated, its preservation is frequently emphasized in contemporary root canal preparation strategies[36]. In mandibular molars, assessing dentine thickness in the pericervical area is particularly important because this region is highly susceptible to structural weakening during root canal preparation, especially in the danger zone of mesial roots, where excessive dentine removal can significantly increase the risk of vertical root fractures and compromise long-term tooth survival[31,32]. In the present study, sequential instrumentation with

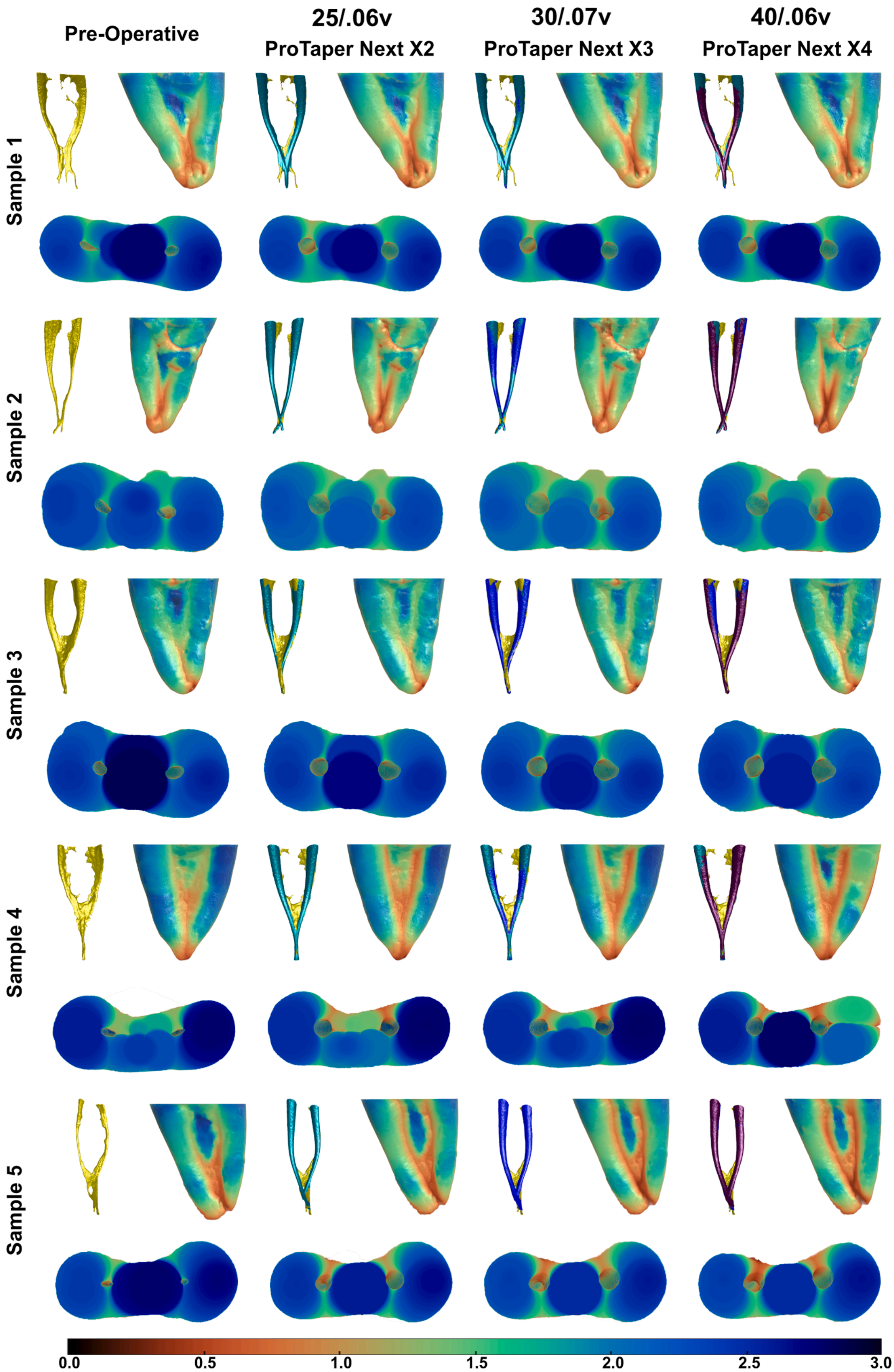

FIGURE 3 – Three-dimensional reconstructions of five mesial roots. Each 3D root canal model shows the canal shape before instrumentation (*yellow*) and after sequential use of 25/.06v (*green*), 30/.07v (*blue*), and 40/.06v (*purple*) instruments. Color-coded 3D root models illustrate external dentine thickness from a distal view, while 2D axial views at 1 mm below the furcation show dentine thickness before and after preparation. Unprepared areas (*yellow*) remain after the final instrument, and dentine thickness decreases progressively with each instrumentation step.

TABLE 2 - Mean and Standard Deviation [Minimum and Maximum Values] of Minimal Dentine Thickness (mm), and Corresponding Percentage Reduction (%) Relative to Preoperative Values, Measured at the Furcation Level and at 1 mm Intervals up to 4 mm Apically (Pericervical Region) in the Mesiobuccal and Mesiolingual Canals of Mandibular Molars, Before and After Sequential Enlargement With Three Rotary Instruments of Increasing Size

Root canal	Preoperative	ProTaper next X2 25/.06v	% reduction	ProTaper next X3 30/.07v	% reduction	ProTaper next X4 40/.06v	% reduction
Furcation level							
Mesiobuccal	$1.55^{a} \pm 0.27$ [1.01-2.01]	$1.18^{b} \pm 0.30$ [0.60-1.72]	25.31 ± 8.20	$1.07^{c} \pm 0.30$ [0.53-1.65]	32.16 ± 9.34	$1.01^{d} \pm 0.30$ [0.41-1.52]	36.39 ± 10.73
Mesiolingual	$1.58^{a} \pm 0.29$ [1.12-2.00]	$1.19^{b} \pm 0.31$ [0.70-1.80]	24.95 ± 9.75	$1.07^{c} \pm 0.31$ [0.67-1.69]	32.83 ± 9.07	$0.99^{d} \pm 0.30$ [0.61-1.56]	37.91 ± 10.34
1 mm							
Mesiobuccal	$0.99^{a} \pm 0.20$ [0.73-1.33]	$0.76^{b} \pm 0.23$ [0.37-1.10]	24.00 ± 11.42	$0.66^{c} \pm 0.21$ [0.31-0.98]	35.08 ± 10.63	$0.60^{d} \pm 0.20$ [0.25-0.90]	40.45 ± 11.08
Mesiolingual	$1.01^{a} \pm 0.22$ [0.67-1.47]	$0.74^{b} \pm 0.20$ [0.37-1.08]	27.83 ± 9.29	$0.65^{c} \pm 0.22$ [0.29-1.00]	37.23 ± 10.49	$0.60^{c} \pm 0.21$ [0.27-1.00]	42.24 ± 10.60
2 mm							
Mesiobuccal	$1.00^{a} \pm 0.20$ [0.75-1.29]	$0.75^{b} \pm 0.19$ [0.43-1.04]	25.54 ± 9.03	$0.68^{c} \pm 0.23$ [0.31-1.02]	32.98 ± 12.46	$0.62^{d} \pm 0.19$ [0.31-0.90]	39.40 ± 10.37
Mesiolingual	$0.99^{a} \pm 0.25$ [0.57-1.39]	$0.73^{b} \pm 0.20$ [0.45-1.04]	26.59 ± 6.95	$0.66^{c} \pm 0.20$ [0.35-0.96]	34.84 ± 6.62	$0.61^{d} \pm 0.20$ [0.33-0.92]	39.51 ± 6.47
3 mm							
Mesiobuccal	$0.99^{a} \pm 0.26$ [0.69-1.57]	$0.82^{b} \pm 0.28$ [0.53-1.47]	18.89 ± 9.23	$0.73^{c} \pm 0.29$ [0.45-1.41]	28.27 ± 10.30	$0.66^{d} \pm 0.30$ [0.37-1.41]	35.86 ± 13.69
Mesiolingual	$0.93^{a} \pm 0.20$ [0.67-1.33]	$0.75^{b} \pm 0.21$ [0.47-1.14]	20.35 ± 7.41	$0.65^{c} \pm 0.17$ [0.41-1.06]	29.72 ± 6.61	$0.59^{d} \pm 0.18$ [0.35-0.98]	37.64 ± 7.21
4 mm							
Mesiobuccal	$0.97^{a} \pm 0.26$ [0.51-1.37]	$0.83^{b} \pm 0.20$ [0.43-1.04]	12.98 ± 8.13	$0.75^{c} \pm 0.20$ [0.37-1.00]	22.04 ± 7.45	$0.71^{c} \pm 0.21$ [0.37-0.98]	27.04 ± 11.14
Mesiolingual	$0.85^{a} \pm 0.20$ [0.55-1.26]	$0.73^{b} \pm 0.19$ [0.43-1.04]	14.47 ± 7.05	$0.66^{c} \pm 0.18$ [0.37-0.98]	23.12 ± 5.27	$0.63^{d} \pm 0.19$ [0.35-0.98]	27.45 ± 6.69
Pericervical region (Furcation to 4 mm)							
Mesiobuccal	1.10 ± 0.33 [0.51-2.01]	0.87 ± 0.29 [0.37.1.72]	21.34 ± 10.57	0.78 ± 0.29 [0.31-1.65]	30.11 ± 11.27	0.72 ± 0.29 [0.25-1.53]	35.83 ± 12.52
Mesiolingual	1.07 ± 0.35 [0.55-2.00]	0.83 ± 0.29 [0.37-1.80]	22.84 ± 9.62	0.74 ± 0.28 [0.29-1.69]	31.55 ± 9.34	0.68 ± 0.27 [0.27-1.56]	36.95 ± 9.94

Different superscript letters in the same line represent statistically significant differences ($P < .05$) between instruments.

progressively larger ProTaper Next instruments (25/.06v, 30/.07v, and 40/.06v) resulted in a mean reduction in dentine thickness at the furcation level from 1.55 mm to 1.01 mm in MB canals and from 1.58 mm to 0.99 mm in ML canals (Table 1; Figs. 3 and 4). This decreasing trend extended up to 4 mm below the furcation, with the most pronounced reduction occurring at the 1 mm and 2 mm levels (Table 2), likely due to the brushing motion recommended by the manufacturer.

The optimal residual dentine thickness at the pericervical area required to prevent root fracture or strip perforation remains poorly defined in the literature. Some authors have proposed critical thresholds below 0.3 mm[37] and 0.5 mm[38] as the minimum value to maintain mechanical resistance. A finite element analysis further substantiates these concerns, demonstrating that reduced residual dentine thickness increases tensile stress and, consequently, the risk of root fracture[33]. To minimize stress concentrations, the authors recommend maintaining a minimum dentine thickness of 0.6 to 0.9 mm in the mesiodistal direction. In another study, Silva et al.[32] reported a significant association between dentine thicknesses ≤1.3 mm and an increased risk of vertical root fracture. However, this latter threshold appears excessively conservative. In the present study, analysis of the dentine thickness distribution across all samples (Fig. 4) revealed that 90.4% of the measurements (n = 362) were already below 1.3 mm, including 16% derived from unprepared root canals. This suggests that the 1.3 mm value may overestimate the clinical risk. While all of these thresholds remain arbitrary and lack definitive clinical validation, a value of 0.5 mm was adopted in this study as the cut-off for residual dentine thickness. Our multimethod evaluation confirmed that while apical enlargement enhanced both shaping outcomes and irrigant effectiveness, it concurrently led to increased dentine removal, with a substantial number of evaluated cross-sections (26%) exhibiting residual dentine thicknesses below 0.5 mm in both the MB and ML canals (Table 3). These findings highlight the trade-off between improved debridement and structural preservation. Consequently, maintaining an adequate dentine thickness should be regarded as a critical parameter in endodontic protocols to ensure that the benefits of enhanced cleaning do not come at the expense of root integrity and long-term tooth survival. It is important to acknowledge that these findings must be interpreted in the context of the specific characteristics of the ProTaper Next system, particularly its

TABLE 3 - Number of Cross-Sections (and Corresponding Percentage Frequencies) Evaluated for Each Canal Before and After Each Preparation Step, Based on Minimum Dentine Thickness on the Distal Aspect of the Mesial Root

Dentine thickness		Mesiobuccal canal	Mesiolingual canal
> 1 mm	Before preparation	28 (56%)	24 (48%)
	After 25/.06v	17 (34%)	14 (28%)
	After 30/.07v	7 (14%)	6 (12%)
	After 40/.06v	6 (12%)	4 (8%)
0.5–1.0 mm	Before preparation	22 (44%)	26 (52%)
	After 25/.06v	30 (60%)	30 (60%)
	After 30/.07v	34 (68%)	34 (68%)
	After 40/.06v	31 (62%)	33 (66%)
< 0.5 mm	Before preparation	0 (0%)	0 (0%)
	After 25/.06v	3 (6%)	6 (12%)
	After 30/.07v	9 (18%)	10 (20%)
	After 40/.06v	13 (26%)	13 (26%)

proprietary alloy, off-centered rectangular cross-sectional design, and progressive taper. These features may contribute to a more aggressive dentine removal pattern for larger instruments, potentially amplifying the reduction in residual dentine thickness observed in this study.

In the literature, several studies evaluating dentine removal during root canal preparation in molars reported only absolute dentine thickness values before and after instrumentation[39-42]. While informative, absolute values alone may not adequately reflect the clinical significance of dentine loss, particularly given the inherent anatomical variability among specimens. In this context, expressing dentine removal as a percentage reduction relative to the original thickness, as performed in this study, provides a more standardized and meaningful metric[17]. This approach allows for more accurate comparisons between samples with differing baseline dimensions. For instance, a uniform reduction of 0.3 mm may appear comparable across specimens, yet it corresponds to a 30% loss in a region with an initial thickness of 1.0 mm, whereas it represents a critical 50%

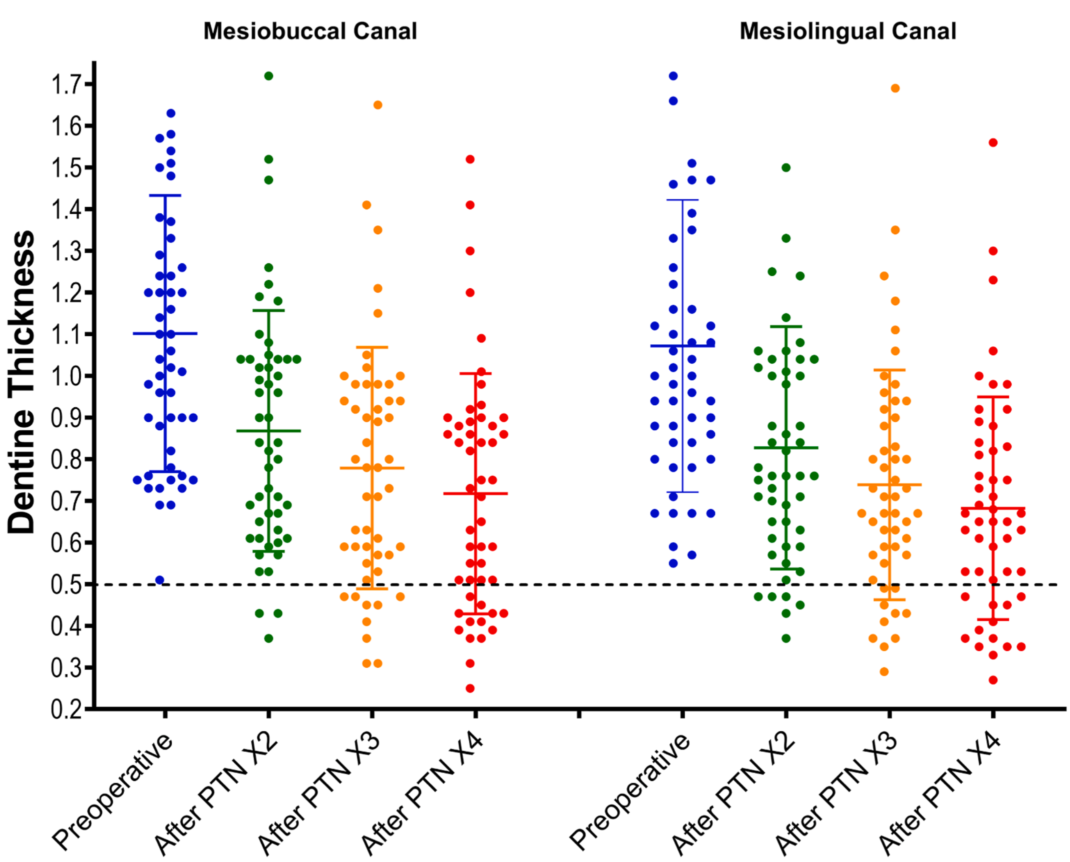

FIGURE 4 – Distribution plot of dentine thickness values measured on the distal aspect of the mesiobuccal and mesiolingual root canals, at 1.0 mm intervals from the furcation level up to 4 mm apically (pericervical area), before and after canal preparation with ProTaper Next (PTN) instruments X2 (25/.06v), X3 (30/.07v), and X4 (40/.06v).

loss in an area starting with only 0.6 mm. This example underscores how identical absolute reductions can have markedly different biomechanical implications, especially in thinner, more vulnerable root regions.

Although root canal preparation has been the most-cited keyword in micro-CT endodontic research over the past 25 years[19], few studies have examined how stepwise enlargement impacts the mesial roots of mandibular molars. To address this gap, the present study evaluated shaping outcomes in MB and ML canals following sequential instrumentation with three ProTaper Next sizes: 25/.06v, 30/.07v, and 40/.06v. Remarkably, only one previous micro-CT study assessed the reduction of dentine thickness in the pericervical area after preparation with the ProTaper Next system[39]. However, comparison with the present study is limited because that study reported only absolute values and measured thickness only after preparation with X3 instrument. They found mean distal dentine thicknesses in the MB and ML canals decreased from 1.16 mm and 1.19 mm (before preparation) to 0.94 mm and 0.98 mm (after X3), corresponding to reductions of approximately 19.0% and 17.6%, respectively. They also noted no dentine thinner than 0.5 mm before preparation and only 1.5% of samples below this threshold after X3. These values contrast with our results, where the mean percentage reduction after X3 was approximately 30% (Table 2), and about 20% of canals showed dentine thickness under 0.5 mm (Table 3, Fig. 4). This discrepancy likely reflects differences in baseline dentine thickness between samples, highlighting the variability of root morphology in this group of teeth. These findings also highlight the complexity of assessing dentine thickness changes and emphasize the importance of reporting both absolute values and percentage reductions to provide a more comprehensive and standardized evaluation of dentine removal during canal preparation.

The evaluation of untouched canal walls (or unprepared canal areas) is also essential when assessing the shaping ability of NiTi instruments, as it reveals areas that remain uncleaned and may harbor debris or bacteria[4]. This helps determine the effectiveness of canal preparation and guides improvements in instrument design and technique. The present stepwise approach findings show a significant increase in intracanal volume and surface area, along with a progressive reduction in unprepared canal walls (Table 1). Micro-CT studies consistently demonstrate that a substantial portion of the canal wall surface area remains untouched following preparation of the mesial root canals of mandibular molars with the ProTaper Next system. Quantitative data from several investigations indicate that the percentage of unprepared or untouched canal walls after ProTaper Next instrumentation generally ranges from approximately 31% to 41%. For example, one micro-CT study evaluating moderately curved mesial canals reported that approximately 31% of the total canal surface area remained untouched, with 14% of the walls unprepared in the apical 5 mm segment[43]. Other comparative studies found that ProTaper Next performed similarly to other contemporary systems in terms of untouched canal wall percentage, with values falling within the same range[44,45]. Additional investigations have corroborated these observations, consistently reporting untouched surface areas between 31% and 41%[46,47]. In the present study, the percentage of untouched canal surface area decreased markedly from 18.07% (25/.06v instrument) to 7.15% after enlargement to a 40/.06v size (Table 1). These values are considerably lower than the mean percentages reported in the literature. Such discrepancies may be attributed to differences in study design, including sample selection, degrees of canal curvature, anatomical variability among specimens, as well as variations in methodological parameters and evaluation criteria used to define and quantify untouched surfaces. However, taken together, findings derived from high-resolution three-dimensional analyses, underscore a critical limitation of current mechanical instrumentation: its inability to fully contact and shape the entire canal surface, particularly in anatomically complex regions such as the mesial roots of mandibular molars.

While mechanical instrumentation influences the extent of canal wall preparation, effective disinfection also depends on irrigant flow dynamics. The present CFD analysis offers complementary insight into how needle design and root anatomy affect apical irrigant penetration and flow behavior. Consistent with previous findings[7], the results showed that open-ended needles provided superior apical penetration compared to side-vented designs across all preparation sizes. The restricted apical flow observed with side-vented needles, especially in the presence of a second canal that diverts irrigant after the needle outlet, limited irrigant delivery to the WL, even after enlargement. In contrast, the open-ended needle achieved deeper apical penetration, likely favored by the anatomical configuration and extending up to the confluence zone[7]. Given that the confluence in this study occurred approximately 1 mm short of the WL, this may explain the irrigant's ability to reach the apex even after a 25/.06v preparation, surpassing outcomes reported in previous studies[7,48]. Although root canal enlargement did not markedly enhance irrigant penetration, it did increase apical flow velocity and density, potentially boosting the advective transport and mechanical action of irrigation. However, this improved delivery with open-ended needles also resulted in higher apical pressures and a correspondingly greater risk of irrigant extrusion compared to side-vented needles, aligning with earlier findings[49]. Although open-ended needles are less frequently recommended in current clinical protocols due to their higher extrusion risk, they remain in use in some settings. In this study, they were included primarily as a reference standard to benchmark CFD simulations and to broaden the analysis of how preparation size influences irrigation dynamics. Nonetheless, it should be noted that in clinical practice, reaching these depths in curved canals may be challenging, and alternatives such as 31-G or polypropylene needles could be considered[48].

The present results also demonstrated that the wall shear stress, an important mechanical factor in biofilm disruption, increased with canal enlargement, contrasting with previous findings from simulations in straight, isolated canals[50,51]. This discrepancy likely results from canal curvature, which redirected the irrigant jet, particularly from the open-ended needle, toward the opposite wall (Fig. 1*B*), unlike in straight canals where flow disperses centrally and uniformly. Furthermore, the use of three anatomical models derived from the same tooth, potentially modified by debris accumulation or removal during preparation, may have brought the needle outlet closer to the canal wall as enlargement progressed, thereby increasing peak wall shear stress. This contrasts with previous studies that used idealized, symmetrical models where enlargement predictably increased the distance between the needle and canal walls[50,51]. These findings underscore that wall shear stress is not determined solely by enlargement but also by anatomical complexity, including curvature, irregularities, and the presence of fins or isthmuses, and by the spatial relationship of the needle to the canal walls. Such variables are difficult to control clinically, and needle positioning is rarely centered, unlike in controlled CFD models. Therefore, in clinical practice, wall shear stress is unlikely to increase predictably with enlargement but instead varies depending on canal-specific anatomy.

Although this study employed the ProTaper Next system, its selection was strategic, as the system embodies several core features common to many contemporary NiTi rotary instruments namely, continuous rotation, standardized apical sizing, variable taper configurations, and the use of heat-treated alloys. These shared design and operational characteristics enhance the relevance of the findings beyond a single system. Moreover, ProTaper Next's widespread clinical adoption and extensive documentation in the literature further support its use as a representative model for investigating the impact of root canal enlargement on shaping efficacy and irrigant dynamics. Therefore, while the results are specific to ProTaper Next, the fundamental insights may be cautiously extrapolated to other systems with similar mechanical and metallurgical properties. In this context, the inclusion of the X4 file (40/.06v) was a deliberate methodological choice to examine the upper limits of apical enlargement under controlled conditions. All instruments used (X2, X3, and X4) were confirmed, through SEM, EDS, and DSC analyses (Fig. 2), to have identical design and alloy properties, differing only in size and taper. This verification was essential to strengthen the internal validity of the study, ensuring that observed differences in shaping and irrigation performance could be confidently attributed to instrument dimensions rather than variability in manufacturing or material composition. Rather than serving as a clinical recommendation, the use of X4 defined the experimental endpoint, allowing a systematic assessment of the point at which further enlargement may compromise structural integrity. This approach aligns with minimally invasive endodontics by helping clinicians recognize when additional enlargement offers limited benefit or potential harm.

With regard to which instrument provided the most favorable balance between shaping efficacy and irrigation performance, the findings of the present study suggest that the 25/.06v instrument represents the most clinically advantageous option. Although the 40/.06v demonstrated slightly better performance in irrigation dynamics, these gains can also be achieved through alternative clinical strategies, such as enhanced irrigant activation or optimized needle design. Moreover, the marginal improvement in unprepared canal surfaces with the 40/.06v (7.15%) compared to the 30/.07v (8.72%) came at the cost of a considerable increase in the proportion of sections with dentine thickness below 0.5 mm (26%), a value associated with a significantly increased risk of root fracture, thus making it unsuitable as a primary clinical goal. Between the 25/.06v and 30/.07v, only minor differences were noted in irrigation performance, indicating that clinical decision-making should primarily consider shaping outcomes. Although the 30/.07v reduced unprepared surface areas from 18.07% to 8.72%, this result should be interpreted in the context of previous studies using similar methodologies, which reported unprepared surface areas between 31% and 41% in comparable roots[46,47]. Thus, the 18.07% of unprepared canal walls observed with the 25/.06v instrument already represents a highly acceptable outcome, particularly considering the complex anatomy of mesial root canals in mandibular molars. Additionally, the proportion of cross-sections with dentine thickness below 0.5 mm was less than half in the 25/.06v group compared to the 30/.07v, further supporting its superior performance in preserving root structure. Therefore, among the instruments tested, the 25/.06v demonstrated the most favorable balance between shaping effectiveness and dentine preservation.

The present study employed a robust methodological design, integrating micro-CT and CFD to comprehensively assess the impact of root canal enlargement in mandibular molars. Although the use of a limited sample size and standardized canal anatomy may restrict the generalizability of the results to broader clinical scenarios, the use of extracted human teeth enhances the external validity. At the same time, the combination of anatomical standardization, high-resolution imaging, and validated CFD modelling strengthens internal validity. While the findings provide meaningful insights into shaping efficacy, dentine preservation, and irrigant dynamics, they are most directly applicable to similar anatomical configurations and instrumentation systems. Future studies should incorporate greater anatomical variability and clinically relevant conditions, such as pulp calcifications, apical deltas, and accessory canals, to improve translational relevance and broaden clinical applicability.

CONCLUSIONS

This study demonstrated that progressive canal enlargement with ProTaper Next system significantly improved shaping outcomes and irrigant dynamics by reducing untouched canal areas and increasing wall shear stress. However, these benefits came at the cost of substantial dentine removal, particularly in the distal aspect of the pericervical region of mesial roots, where structural preservation is critical. Open-ended needles consistently achieved deeper irrigant penetration to the WL compared to side-vented designs, regardless of the preparation size. While larger apical sizes enhanced irrigation efficiency, they also elevated the risk of weakening the root, especially in anatomically vulnerable areas. These findings underscore the importance of tailoring canal enlargement to each anatomy, balancing the need for effective debridement with the preservation of dentinal structure to minimize the risk of structural failure.

ACKNOWLEDGEMENTS

The authors acknowledge Francisco Manuel Braz Fernandes and Fernanda Carvalho for running the differential scanning calorimetry tests on the endodontic instruments. The authors also acknowledge Daniel Janeiro and Carolina Mendes from S3D for conducting the optical 3D scannings.

The authors deny any conflicts of interest.

REFERENCES

1. Barbosa-Ribeiro M, Arruda-Vasconcelos R, Louzada LM, et al. Microbiological analysis of endodontically treated teeth with apical periodontitis before and after endodontic retreatment. Clin Oral Investig 2021;25:2017–27.

2. Pinto KP, Barbosa AFA, Silva E, et al. What is the microbial profile in persistent endodontic infections? A scoping review. J Endod 2023;49:786–98.

3. Versiani MA, Martins J, Ordinola-Zapata R. Anatomical complexities affecting root canal preparation: a narrative review. Aust Dent J 2023;68(Suppl 1):S5–23.
4. Siqueira JF Jr, Perez AR, Marceliano-Alves MF, et al. What happens to unprepared root canal walls: a correlative analysis using micro-computed tomography and histology/scanning electron microscopy. Int Endod J 2018;51:501–8.
5. Siqueira Junior JF, Rocas IDN, Marceliano-Alves MF, et al. Unprepared root canal surface areas: causes, clinical implications, and therapeutic strategies. Braz Oral Res 2018;32:e65.
6. Boutsioukis C, Gogos C, Verhaagen B, et al. The effect of apical preparation size on irrigant flow in root canals evaluated using an unsteady computational fluid dynamics model. Int Endod J 2010;43:874–81.
7. Rito Pereira M, Silva G, Semiao V, et al. Syringe irrigation in confluent canals: a sequential computational fluid dynamics assessment. Aust Endod J 2024;50:40–51.
8. de Gregorio C, Arias A, Navarrete N, et al. Effect of apical size and taper on volume of irrigant delivered at working length with apical negative pressure at different root curvatures. J Endod 2013;39:119–24.
9. Rodrigues RCV, Zandi H, Kristoffersen AK, et al. Influence of the apical preparation sze and the irrigant type on bacterial reduction in root canal-treated teeth with apical periodontitis. J Endod 2017;43:1058–63.
10. Fornari VJ, Silva-Sousa YT, Vanni JR, et al. Histological evaluation of the effectiveness of increased apical enlargement for cleaning the apical third of curved canals. Int Endod J 2010;43:988–94.
11. Aminoshariae A, Kulild JC. Master apical file size - smaller or larger: a systematic review of healing outcomes. Int Endod J 2015;48:639–47.
12. Sabeti MA, Saqib Ihsan M, Aminoshariae A. The effect of master apical preparation size on healing outcomes in endodontic treatment: a systematic review and meta-analysis. J Endod 2024;50:292–8.
13. Keleş A, Keskin C, Karataslioglu E, et al. Middle mesial canal preparation enhances the risk of fracture in mesial root of mandibular molars. J Endod 2020;46:1323–9.
14. Pauletto G, Soares PM, Baumhardt T, et al. Effect of radiotherapy and taper of root canal preparation on the biomechanical behavior of mesial roots of mandibular molars. J Endod 2024;50:827–34.
15. Smoljan M, Hussein MO, Guentsch A, Ibrahim M. Influence of progressive versus minimal canal preparations on the fracture resistance of mandibular molars: a 3-dimensional finite element analysis. J Endod 2021;47:932–8.
16. Lee OYS, Khan K, Li KY, et al. Influence of apical preparation size and irrigation technique on root canal debridement: a histological analysis of round and oval root canals. Int Endod J 2019;52:1366–76.
17. De-Deus G, Rodrigues EA, Lee JK, et al. Taper 0.06 versus Taper 0.04: the impact on the danger zone. J Endod 2023;49:536–43.
18. Gulabivala K, Patel B, Evans G, Ng Y-L. Effects of mechanical and chemical procedures on root canal surfaces. Endod Top 2005;10:103–22.
19. Aksoy U, Kucuk M, Versiani MA, Orhan K. Publication trends in micro-CT endodontic research: a bibliometric analysis over a 25-year period. Int Endod J 2021;54:343–53.
20. Barbosa AFA, de Lima CO, Antunes BR, et al. Effect of the progressive taper enlargement of buccal root canals of three-rooted maxillary molars: a stepwise micro-CT study. Aust Endod J 2023;49:700–10.
21. Ordinola-Zapata R, Martins JNR, Versiani MA, Bramante CM. Micro-CT analysis of danger zone thickness in the mesiobuccal roots of maxillary first molars. Int Endod J 2019;52:524–9.
22. Rito PM, Morouço P, Vasconcelos I, et al. Computer fluid dynamics as a tool for analysis of endodontic irrigation. AIP Conf Proc 2018;1978:160003.
23. Tomaszewska IM, Skinningsrud B, Jarzebska A, et al. Internal and external morphology of mandibular molars: an original micro-CT study and meta-analysis with review of implications for endodontic therapy. Clin Anat 2018;31:797–811.
24. Sousa-Neto MD, Silva-Sousa YC, Mazzi-Chaves JF, et al. Root canal preparation using micro-computed tomography analysis: a literature review. Braz Oral Res 2018;32:e66.

25. ASTM International. ASTM F2004−17: Standard Test Method For Transformation Temperature of Nickel-Titanium Alloys by Thermal Analysis. West Conshohocken, PA: American Society for Testing and Materials; 2004.

26. Rito Pereira M, Silva G, Semiao V, et al. Experimental validation of a computational fluid dynamics model using micro-particle image velocimetry of the irrigation flow in confluent canals. Int Endod J 2022;55:1394–403.

27. Guerisoli DMZ, Silva RS, Pécora JD. Evaluation of some physico-chemical properties of different concentrations of sodium hypochlorite solutions. Braz Endod J 1998;3:21–3.

28. Paqué F, Ganahl D, Peters OA. Effects of root canal preparation on apical geometry assessed by micro-computed tomography. J Endod 2009;35:1056–9.

29. Hülsmann M, Peters OA, Dummer PMH. Mechanical preparation of root canals: shaping goals, techniques and means. Endod Top 2005;10:30–76.

30. Boutsioukis C, Arias-Moliz MT. Present status and future directions - irrigants and irrigation methods. Int Endod J 2022;55:588–612.

31. ElAyouti A, Connert T, Dummer P, Löst C. A critical analysis of research methods and experimental models to study working length determination and the performance of apex locators – a narrative review with recommendations for the future. Int Endod J 2022;55:281–94.

32. Silva LR, de Lima KL, Santos AA, et al. Dentin thickness as a risk factor for vertical root fracture in endodontically treated teeth: a case-control study. Clin Oral Investig 2021;25:1099–105.

33. Wang ZF, Fu BP. Minimum residual root dentin thickness of mandibular premolars restored with a post: a finite element analysis study. J Prosthet Dent 2024;131:878–85.

34. Ng YL, Mann V, Gulabivala K. A prospective study of the factors affecting outcomes of nonsurgical root canal treatment: part 1: periapical health. Int Endod J 2011;44:583–609.

35. Clark D, Khademi J. Modern molar endodontic access and directed dentin conservation. Dent Clin North Am 2010;54:249–73.

36. Bóveda C, Kishen A. Contracted endodontic cavities: the foundation for less invasive alternatives in the management of apical periodontitis. Endod Top 2015;33:169–86.

37. Lim SS, Stock CJ. The risk of perforation in the curved canal: anticurvature filing compared with the stepback technique. Int Endod J 1987;20:33–9.

38. Elayouti A, Chu AL, Kimionis I, et al. Efficacy of rotary instruments with greater taper in preparing oval root canals. Int Endod J 2008;41:1088–92.

39. Keleş A, Keskin C, Alqawasmi R, Versiani MA. Evaluation of dentine thickness of middle mesial canals of mandibular molars prepared with rotary instruments: a micro-CT study. Int Endod J 2020;53:519–28.

40. Silva RV, Alcalde MP, Horta MC, et al. Root canal shaping of curved canals by Reciproc blue system and pro taper gold: a micro-computed tomographic study. J Clin Exp Dent 2021;13:e112–8.

41. Santos-Junior AO, Fontenele RC, Tavares K, et al. Effectiveness and safety of three NiTi systems in endodontic retreatment of MB1 and MB2 root canals: a micro-CT and CBCT combined analysis. Clin Oral Investig 2025;29:194.

42. Gao Y, Shen Y, Zhou X, Haapasalo M. Remaining root dentin thickness in mesiobuccal canals of maxillary first molars after attempted removal of broken instrument fragments. Austr Endod J 2015;41:122–7.

43. Brasil SC, Marceliano-Alves MF, Marques ML, et al. Canal transportation, unprepared areas, and dentin removal after preparation with BT-RaCe and ProTaper Next systems. J Endod 2017;43:1683–7.

44. Drukteinis S, Peciuliene V, Dummer PMH, Hupp J. Shaping ability of BioRace, ProTaper NEXT and genius nickel-titanium instruments in curved canals of mandibular molars: a MicroCT study. Int Endod J 2019;52:86–93.

45. da Silva Limoeiro AG, Dos Santos AH, De Martin AS, et al. Micro-computed tomographic evaluation of 2 nickel-titanium instrument systems in shaping root canals. J Endod 2016;42:496–9.

46. Yanik D, Ozel S. Shaping ability of three instrumentation system in moderately curved canals: a micro-CT study. Microsc Res Tech 2024;87:2399–407.

47. Gagliardi J, Versiani MA, de Sousa-Neto MD, et al. Evaluation of the shaping characteristics of ProTaper Gold, ProTaper NEXT, and ProTaper universal in curved canals. J Endod 2015;41:1718–24.

48. Boutsioukis C, Gutierrez NP. Syringe irrigation in minimally shaped root canals using 3 endodontic needles: a computational fluid dynamics study. J Endod 2021;47:1487–95.

49. Boutsioukis C, Gogos C, Verhaagen B, et al. The effect of root canal taper on the irrigant flow: evaluation using an unsteady computational fluid dynamics model. Int Endod J 2010;43:909–16.

50. Boutsioukis C, Lambrianidis T, Verhaagen B, et al. The effect of needle-insertion depth on the irrigant flow in the root canal: evaluation using an unsteady computational fluid dynamics model. J Endod 2010;36:1664–8.

51. Boutsioukis C, Verhaagen B, Versluis M, et al. Evaluation of irrigant flow in the root canal using different needle types by an unsteady computational fluid dynamics model. J Endod 2010;36:875–9.